Pressure-induced phase transitions in nanocrystalline ReO_3

2007 J. Phys.: Condens. Matter 19 436214

(http://iopscience.iop.org/0953-8984/19/43/436214)

J. Phys.: Condens. Matter **19** (2007) 436214 (11pp) doi:10.1088/0953-8984/19/43/436214

Pressure-induced phase transitions in nanocrystalline ReO_3

Kanishka Biswas[1,2], D V S Muthu[3], A K Sood[1,3], M B Kruger[4], B Chen[5] and C N R Rao[1,2,6]

[1] Chemistry and Physics of Materials Unit, DST Unit on Nanoscience and CSIR Centre of Excellence in Chemistry, Jawaharlal Nehru Centre for Advanced Scientific Research, Jakkur PO, Bangalore 560064, India
[2] Solid State and Structural Chemistry Unit, Indian Institute of Science, Bangalore 560012, India
[3] Department of Physics, Indian Institute of Science, Bangalore 560012, India
[4] Department of Physics, University of Missouri, Kansas City, MO 64110, USA
[5] Department of Earth and Planetary Science, University of California, Berkeley, CA 94720, USA

E-mail: cnrrao@jncasr.ac.in

Received 28 June 2007, in final form 10 September 2007
Published 28 September 2007
Online at stacks.iop.org/JPhysCM/19/436214

Abstract

Pressure-induced phase transitions in the nanocrystals of ReO_3 with an average diameter of ∼12 nm have been investigated in detail by using synchrotron x-ray diffraction and the results compared with the literature data of bulk samples of ReO_3. The study shows that the ambient-pressure cubic I phase (space group $Pm\bar{3}m$) transforms to a monoclinic phase (space group $C2/c$), then to a rhombohedral I phase (space group $R\bar{3}c$), and finally to another rhombohedral phase (rhombohedral II, space group $R\bar{3}c$) with increasing pressure over the 0.0–20.3 GPa range. The cubic I to monoclinic transition is associated with the largest volume change (∼5%), indicative of a reconstructive transition. The transition pressures are generally lower than those known for bulk ReO_3. The cubic II ($Im\bar{3}$) or tetragonal ($P4/mbm$) phases do not occur at lower pressures. The nanocrystals are found to be more compressible than bulk ReO_3. On decompression to ambient pressure, the structure does not revert back to the cubic I structure.

1. Introduction

ReO_3 is one of the most unusual metal oxides, with a cubic structure and exhibiting metallic conductivity [1, 2]. It is comparable to copper both in its appearance and electronic properties. A pressure-induced phase transition in ReO_3 was first reported by Razavi *et al* [3], who observed an anomalous increase in the Fermi surface cross section above 0.3 GPa. Schirber

[6] Author to whom any correspondence should be addressed.

and Morosin [4] demonstrated that ReO_3 undergoes a second-order phase transition in which the compressibility jumps to a much higher value in the high-pressure phase. The transition was considered to involve a tetragonal distortion accompanying a displacement of the O atoms from the linear O–Re–O chains of the cubic phase to a hinged arrangement. High-precision strain measurements established that ReO_3 undergoes a pressure-induced phase transformation at 0.5 GPa at room temperature [5]. In a neutron scattering study, Axe *et al* [6] observed a softening of an M-type phonon in a single crystal of ReO_3 near the transition. ReO_3 was assigned the space group $Im\bar{3}$ at ∼1.5 GPa, well above the compressibility collapse ($P_c = 0.52$ GPa) [7]. In this structure, the oxygen octahedra are slightly rotated to form a 165° Re–O–Re angle. The $Im\bar{3}$ space group itself was first suggested for the high-pressure phase by Schirber and Mattheiss [8] based on non-structural considerations. Jørgensen *et al* [9] reported a sequence of phase transitions in ReO_3 starting at 0.5 GPa, consistent with the condensation of the M_3 phonon. The structure was cubic $Pm\bar{3}m$ at ambient pressure, tetragonal $P4/mbm$ at 0.52 GPa, and cubic $Im\bar{3}$ at 0.73 GPa and higher pressures. The rotation angle of the ReO_6 octahedra is associated with the distortion in the high-pressure phases. Neutron diffraction studies [10], also suggested the occurrence of the tetragonal phase between the two cubic phases. Based on an energy dispersive synchrotron x-ray diffraction study, Jørgensen *et al* [11] later showed that the $Im\bar{3}$ phase transforms to a MnF_3-related monoclinic phase around 3 GPa, a VF_3-related rhombohedral phase (rhombohedral I) at ∼12.8 GPa, and finally to another rhombohedral phase (rhombohedral II) at ∼39 GPa. By the use of angle-dispersive x-ray powder diffraction Suzuki *et al* [12] have demonstrated the coexistence of cubic $Im\bar{3}$ and the rhombohedral I phase in the 8–18 GPa range. The apparent change in the diffraction pattern observed above 38 GPa was taken to signify the formation of the rhombohedral II phase. Recently, Jørgensen *et al* [13] have shown that the existence of the $Im\bar{3}$ phase in the 0.5–13.2 GPa range by neutron powder time-of-flight diffraction as well as x-ray diffraction by using Fluorinert FC-75 as the pressure transmitting medium. In this study, the monoclinic phase was not found. In spite of several studies, the sequences of pressure-induced transitions of ReO_3 as well as the exact structures of the different phases are not entirely clean. Furthermore, the diffraction data in most of these studies were not subjected to profile analysis.

We have investigated the pressure-induced transitions in ReO_3 nanocrystals prepared by the solvothermal decomposition of the rhenium (VII) oxide–dioxane complex, by synchrotron x-ray diffraction, by carrying out the Rietveld profile analysis of the diffraction patterns. The study carried out over the 0.0–20.3 GPa range, has revealed three phase transitions, all occurring at much lower pressures compared to the bulk. We fail to observe the cubic $Im\bar{3}$ or the tetragonal $P4/mbm$ phase. Furthermore, the transitions are not entirely reversible. Thus, we do not obtain the $Pm\bar{3}m$ cubic phase at ambient pressures on decompression. The cubic to monoclinic transition is associated with the largest change in volume, indicating it to be a generally first-order reconstructive phase transition. The values of the bulk modulus (B_0) of the different phases of the nanocrystals are smaller than those of the bulk.

2. Experimental details

ReO_3 nanocrystals of ∼12 nm diameter were prepared by the decomposition of the Re_2O_7-dioxane complex under solvothermal conditions [14]. The rhenium (VII) oxide–dioxane complex, Re_2O_7–$(C_4H_8O_2)_x$ was prepared by a known procedure [15, 16], and was decomposed in toluene under solvothermal conditions to yield the nanocrystals. In order to prepare the nanocrystals of ∼12 nm diameter, 0.025 g (0.12 mmol) of Re_2O_7 was taken in a 10 ml round-bottomed flask and 0.25 ml (2.93 mmol) of anhydrous 1,4-dioxane was added to it. This mixture was warmed in a water bath maintained at 70 °C and then frozen in an ice bath

alternately until rhenium (VII) oxide–dioxane complex (RDC) precipitated out as a dense, pearl gray deposit. The complex was dissolved in 2 ml (30.08 mmol) of ethanol, the solution added to 45 ml of toluene, and sealed in a Teflon-lined stainless steel autoclave of 80 ml capacity (at 70% filling fraction). The autoclave was heated at 200 °C for 4 h. Copper-red ReO_3 nanocrystals so obtained were washed several times with acetone.

The ReO_3 nanoparticles were characterized by powder x-ray diffraction using a Phillips X'Pert diffractometer employing the Bragg–Brentano configuration. For transmission electron microscopy (TEM), hexane or carbon tetrachloride dispersions of the nanoparticles were taken on holey carbon-coated Cu grids and the grids were left to dry in air. The grids were examined using a JEOL (JEM3010) microscope operating with an accelerating voltage of 300 kV. Electronic absorption spectra were recorded using a Perkin-Elmer spectrometer.

High-pressure x-ray diffraction experiments on the ReO_3 nanocrystals of average diameter $\sim$12 nm were performed in a Mao–Bell-type diamond anvil cell with anvils having 350 μm culets. A spring-steel gasket, with sample chamber having a diameter of $\sim$150 μm, was used to contain the sample. A mixture of 4:1 methanol:ethanol was used as the pressure transmitting medium. In addition, $\sim$5–10 μm ruby spheres were included to determine the pressure using the ruby fluorescence technique [17]. X-ray diffraction data were collected up to 20.3 GPa using a liquid nitrogen cooled Ge detector in energy dispersive mode at beam line X17B3 of the National Synchrotron Light Source, Brookhaven, USA. The detector was positioned $2\theta = 10.0008^\circ \pm 0.002^\circ$. High-pressure synchrotron x-ray patterns were fitted by Rietveld profile matching using FULLPROF suit program [18, 19]. The lattice parameters as well as further non-structural parameters (i.e. background, peak profile parameters including asymmetry) were refined by the profile matching method using the FULLPROF suite. This procedure, also known as LeBail [20] or Pawley-type fitting [21], does not require any structural information except the approximate unit cell and resolution parameters.

3. Results and discussion

In figure 1(a), we show the powder x-ray diffraction pattern of the ReO_3 nanocrystals obtained with the laboratory x-ray diffraction instrument under ambient conditions. The pattern could be indexed on the $Pm\bar{3}m$ space group (JCPDS 00-24-1009). By making use of the line-widths, the average particle size was estimated to be $\sim$12 nm by using the Scherrer formula. A TEM image of a ReO_3 nanocrystal is shown in figure 1(b). The nanocrystals are reasonably monodisperse as seen from the histogram given as the lower inset in the figure 1(b). The upper inset in figure 1(b) shows a high-resolution electron microscope image of a nanocrystal. The lattice spacings of 3.77 and 2.67 Å correspond to the (100) and (110) interplanar distances respectively. ReO_3 is known to exhibit a plasmon absorption band around 520 nm in the electronic absorption spectrum [22]. In figure 1(c), we show the electronic absorption spectrum of the ReO_3 nanocrystals. The spectrum clearly shows an absorption band with a maximum around 507 nm due to plasmon resonance. The band maximum is not that different from that in Au nanocrystals, but the band is broad, extending over the 400–800 nm regions.

Energy dispersive x-ray diffraction patterns were recorded in compression as well as decompression modes in the pressure range 0.0–20.3 GPa. The experimental patterns were subjected to Rietveld profile analysis. In figure 2, we show the experimental (open circles), fitted (solid lines) and difference (dotted lines) diffraction patterns for the different phases in the 0.0–20.3 GPa range.

The x-ray diffraction patterns are generally broad due to the small particle size. On profile analysis, the ambient-pressure pattern (figure 2(a)) could be indexed on the primitive cubic unit cell with the $Pm\bar{3}m$ space group (JCPDS 00-24-1009). The values of the weighted

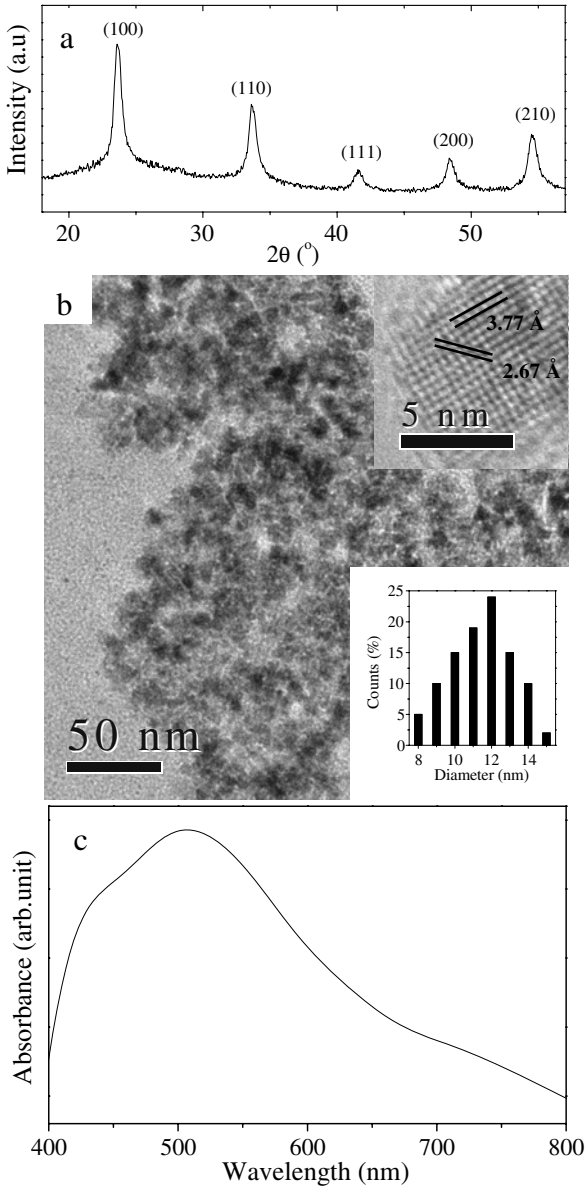

Figure 1. (a) Powder XRD pattern from a Phillips laboratory diffractometer of the ReO_3 nanocrystals (∼12 nm average diameter). (b) TEM image along with size distribution histogram as a lower inset of the same ReO_3 nanocrystals. Upper inset shows a high-resolution TEM image of a nanocrystal. (c) Optical absorption spectrum of the ReO_3 nanocrystals (∼12 nm average diameter).

profile factor (R_{wp}), expected profile factor (R_{exp}), and reduced chi-square (χ^2) obtained were satisfactory (table 1). The lattice parameter obtained from the profile fit is 3.7665 (3) Å. Jørgensen *et al* [11] reported a value of 3.7518 (5) Å for the bulk sample, suggesting a slight increase in the lattice parameter in the nanocrystals due to small particle size. Such an increase in the lattice parameters of nanocrystals has been reported earlier [14, 23, 24].

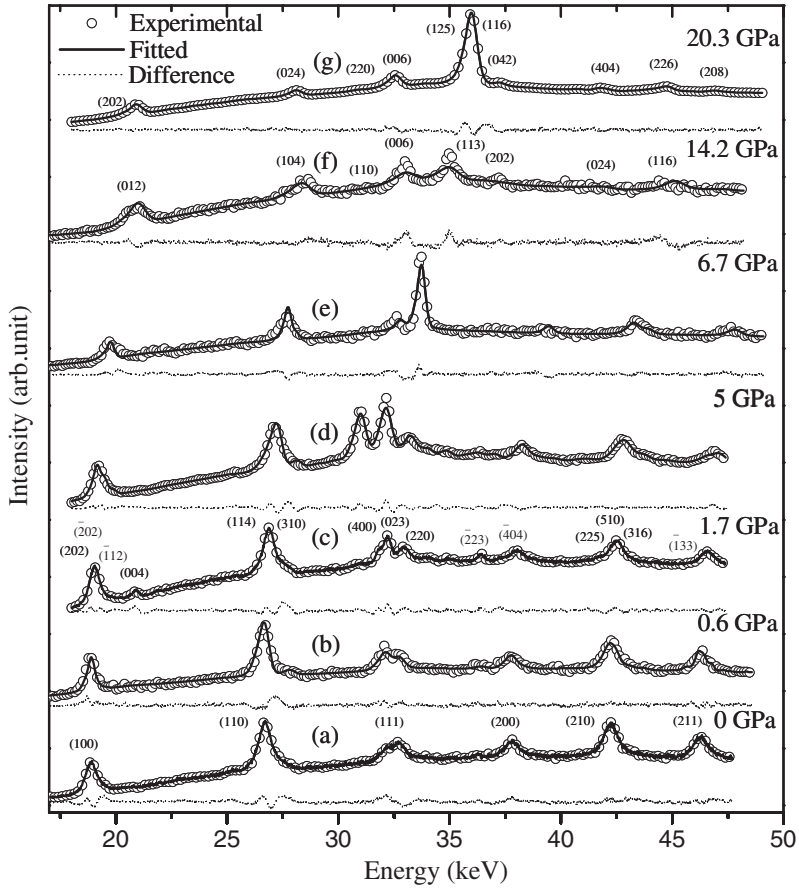

Figure 2. High-pressure energy dispersive experimental XRD patterns of the ∼12 nm ReO_3 nanocrystals along with Rietveld fits and difference patterns at (a) 0.0, (b) 0.6, (c) 1.7, (d) 5, (e) 6.7, (f) 14.2, and (g) 20.3 GPa respectively in the compression process.

The x-ray diffraction patterns recorded in the pressure range 0.3–5 GPa (figures 2(b)–(d)) could be fitted well to a monoclinic structure with the space group $C2/c$ (JCPDS 00-72-1203). In figure 2(c), we have indicated the (hkl) values of the reflections of the monoclinic phase. In figure 3, we show the x-ray diffraction pattern recorded at 0.3 GPa with the fits to cubic I (space group $Pm\bar{3}m$), cubic II (space group $Im\bar{3}$), and monoclinic (space group $C2/c$) structures. We find the best fit for the monoclinic structure, the values of R_{wp}, R_{exp}, and χ^2 for the cubic I, cubic II, and monoclinic phases being 8.43%, 3.78%, 4.97; 8.41%, 3.78%, 4.94, and 5.55%, 3.49%, 2.04 respectively. The lattice parameters of the monoclinic phase are found to be $a = 8.9996(2)$, $b = 4.9440(3)$, $c = 13.6370(3)$ Å, $\beta = 91.0(1)^\circ$ (table 1). The monoclinic phase of bulk ReO_3 is reported to have a MnF_3-related structure (space group $C2/c$) [11, 25]. The MnF_6 octahedra in MnF_3 exhibit Jahn–Teller distortion due to the Mn^{3+} ion with a $3d^4$ high-spin configuration. The Re^{6+} ion has one electron in the t_{2g} orbital and the distortion of the ReO_6 octahedra is expected to be relatively small in comparison with the distortions caused by the e_g electron. It should be recalled that Jørgensen *et al* [9, 11] reported the existence of tetragonal (space group $P4/mbm$) and cubic II (space group $Im\bar{3}$) phases in the 0.5–2.7 GPa range in the case of bulk ReO_3. We do not find evidence for these phases

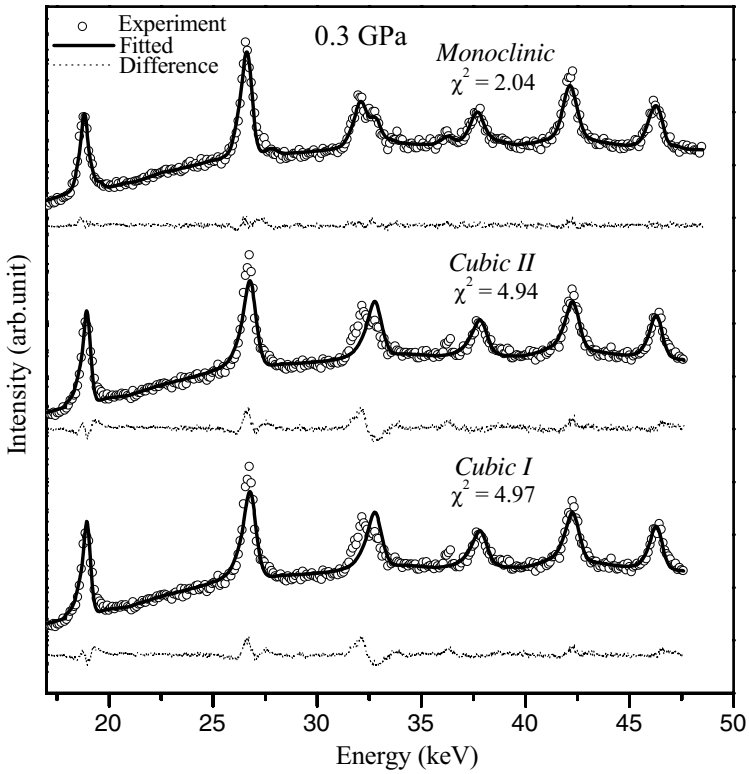

Figure 3. Energy dispersive XRD patterns of the ∼12 nm ReO_3 nanocrystals at 0.3 GPa fitted for cubic I, cubic II, and monoclinic structures.

Table 1. Structural parameters obtained by Rietveld profile analysis of the synchrotron x-ray diffraction data for different pressure-induced phases of ReO_3 nanocrystals.

P (GPa)	Space gr.	a (Å)	b (Å)	c (Å)	β (deg)	Unit cell volume, V (Å^3)	R_{wp}(%)[a]	R_{exp}(%)[b]	χ^{2c}
0	$Pm\bar{3}m$	3.7665 (3)				53.435 (2)	4.70	2.27	2.31
0.3	$C2/c$	8.9996 (2)	4.9440 (3)	13.6370 (3)	91.00 (1)	610.184 (2)	5.55	3.49	2.04
0.6	$C2/c$	8.9768 (3)	4.9693 (4)	13.6369 (4)	90.85 (2)	608.245 (1)	6.02	3.70	2.65
1.0	$C2/c$	8.8622 (3)	4.9692 (2)	13.5595 (4)	91.39 (2)	596.957 (1)	5.55	3.76	2.18
1.7	$C2/c$	8.8696 (3)	4.9440 (3)	13.5160 (3)	91.23 (2)	592.555 (1)	2.74	1.30	1.75
2.6	$C2/c$	8.9439 (3)	4.9215 (3)	13.2503 (3)	90.48 (2)	583.222 (1)	2.84	2.30	1.53
5	$C2/c$	8.8904 (3)	4.8998 (4)	13.2814 (3)	91.02 (2)	578.458 (1)	3.12	1.25	1.84
6.7	$R\bar{3}c$	5.0698 (4)		12.6606 (3)		281.820 (1)	6.61	3.21	4.23
9.8	$R\bar{3}c$	5.0099 (3)		12.4716 (2)		271.092 (2)	7.50	3.24	5.35
14.2	$R\bar{3}c$	4.6238 (3)		12.9556 (2)		239.875 (1)	5.02	3.16	2.52
20.3	$R\bar{3}c$	9.2322 (2)		13.1234 (3)		968.691 (1)	3.87	2.88	1.81

[a] Weighted profile factor.
[b] Expected weighted profile factor.
[c] Reduced chi-square.

in the nanocrystals in this pressure range. By using a 4:1 methanol:ethanol mixture as the pressure-transmitting medium Jørgensen *et al* [11] found a monoclinic phase in the pressure range 3–12 GPa. Jørgensen *et al* [13] have, however, found no evidence for the monoclinic

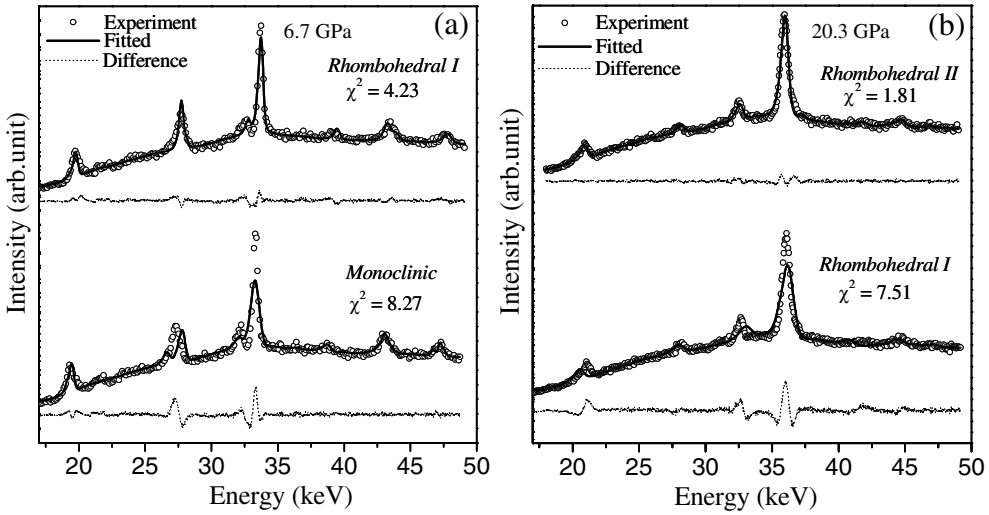

Figure 4. Energy dispersive XRD patterns of the ∼12 nm ReO_3 nanocrystals (a) at 6.7 GPa fitted for monoclinic phase and rhombohedral I phase, and (b) at 20.3 GPa fitted for rhombohedral I and rhombohedral II structures.

phase of ReO_3 by neutron as well as x-ray diffraction measurement when they used Fluorinert FC-75 as the pressure-transmitting medium. It should be noted that we have used the 4:1 methanol:ethanol mixture in the present study. The cubic to monoclinic phase transition found by us in the nanocrystals occurs at a much lower pressure than that reported for the bulk sample.

The x-ray diffraction patterns recorded above 5 GPa could be indexed on rhombohedral unit cells. Figures 2(e)–(f) show the experimental diffraction patterns obtained at 6.7, and 14.2 GPa along with the profile fits to the rhombohedral I (space group $R\bar{3}c$, JCPDS 00-45-1039) structures and along with the difference patterns. We have indicated the (*hkl*) values of the reflections of the rhombohedral I phase in figure 2(f). The monoclinic to rhombohedral I phase transition seems to occur around 6.7 GPa. We have therefore, fitted the experimental diffraction pattern at this pressure for both the structures in figure 4(a). The fit to the rhombohedral I structure is much better than that for the monoclinic structure. The values of R_{wp}, R_{exp}, and χ^2 obtained for the fits to the monoclinic and rhombohedral I structures are 9.32%, 3.24%, 8.27, and 6.61%, 3.21%, 4.23 respectively. The lattice parameters of rhombohedral I phase are $a = b = 5.0698$ (4) and $c = 12.6606$ (3) Å (table 1). Jørgensen *et al* [11] suggested that the high-pressure phase of bulk ReO_3 has the VF_3-type structure (space group $R\bar{3}c$) [26], derived from the cubic ($Pm\bar{3}m$) perovskite structure by a coupled rotation of the corner-linked octahedra around the ⟨111⟩ direction. Assuming no distortion of the octahedra, the volume decreases gradually as the rotation angle in increased. Hexagonal close-packing is achieved when the rotation angle reaches 30°. In bulk ReO_3, Jørgensen *et al* [11] and Suzuki *et al* [12] observed the rhombohedral I phase above 12 and 10.4 GPa respectively. Thus, in the case of the nanocrystals, the monoclinic to rhombohedral phase transition occurs at a much lower pressure.

We could successfully index the diffraction pattern at 20.3 GPa to a second rhombohedral phase, labelled as rhombohedral II with a unit cell four times larger than that of the rhombohedral I (i.e. $2a \times 2b \times c$) as shown in figure 2(g). The symmetry of this phase is not different from that of rhombohedral I. In figure 4(b), we show the fits of the experimental diffraction pattern for the rhombohedral I and rhombohedral II structures. It is clear that the rhombohedral II phase gives a better fit. The values of R_{wp}, R_{exp} and χ^2 obtained from the fits

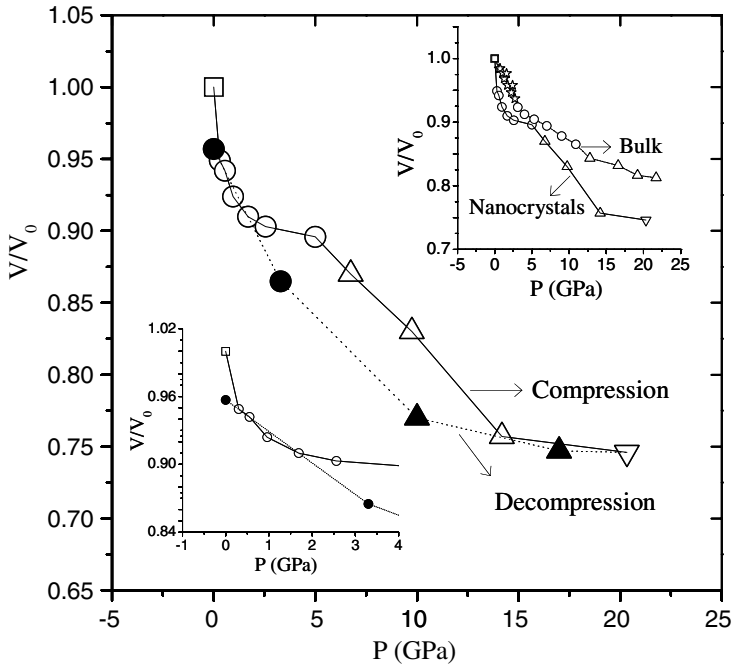

Figure 5. Relative volume versus pressure curve for different phases of ReO_3 nanocrystals in the compression (open symbols) and decompression (filled symbols) experiments in the 0.0–20.3 GPa pressure range. Cubic I (squares), monoclinic (circles), rhombohedral I (triangles), and rhombohedral II (inverted triangles). The top inset compares the phase transition data of the nanocrystals (present study) under compression with the literature data on bulk ReO_3 [9, 11]. Stars are used to represent the cubic II phase identified in the case of the bulk sample. The bottom inset shows the magnified 0.0–4.0 GPa region.

for rhombohedral I and rhombohedral II phases are 8.09%, 2.95%, 7.51, and 3.87%, 2.88%, 1.81 respectively. The lattice parameters obtained from the profile fit for rhombohedral II phase are $a = b = 9.2322$ (2) and $c = 13.1234$ (3) Å (table 1). Jørgensen *et al* [11] and Suzuki *et al* [12] have observed the rhombohedral II phase above 38 GPa in bulk ReO_3. We observe the rhombohedral II phase in the nanocrystals at a much lower pressure.

We have examined the phases of nanocrystalline ReO_3 after decompression. In the decompression process, we find that the rhombohedral II phase transforms back to the rhombohedral I phase around 17 GPa, and remains as rhombohedral I down to 10 GPa. The experimental x-ray diffraction patterns at 17 and 10 GPa could be fitted with the rhombohedral I structure. Further decompression resulted in the transformation of rhombohedral I to monoclinic phase at 3 GPa. Suzuki *et al* [12] observed that the rhombohedral II phase does not transform back to the rhombohedral I phase or to the ambient-pressure cubic phase. We have not found evidence for the cubic phase at ambient pressures after decompression. Although the experimental pattern at ambient pressure (after the decompression) was not too well resolved, it could be best fitted with the monoclinic structure. The values of R_{wp}, R_{exp}, and χ^2 obtained from the fit to the monoclinic structure are 3.28%, 2.33%, 1.98 respectively. In any case, it is certainly not cubic. The fit for the cubic $Pm\bar{3}m$ structure was also not as satisfactory, the values of R_{wp}, R_{exp}, and χ^2 being 13.2%, 8.27%, 34.1 respectively. It is known that metastable phases get stabilized in the nanocrystals of many materials as exemplified by CoO and CdS [27, 28].

We have calculated the unit cell volume of the different phases of nanocrystalline ReO_3 in the 0.0–20.3 GPa range from the profile fits (table 1). Figure 5 shows the plots of the relative

volume against pressure in both the compression (open symbols) and the decompression (filled symbols) processes. The lower inset in figure 5 shows the magnification of the data 0.0–4.0 GPa range. In the top inset in figure 5, we show the plot of the literature values of the relative volume against pressure for the bulk ReO_3 for purpose of comparison. Here, the relative volume is defined as the ratio of the volume per ReO_3 formula unit in each pressure to the volume per ReO_3 formula unit in ambient pressure. We see from figure 5 that there is a discontinuous drop in the relative volume of about 5% in the cubic I (space group $Pm\bar{3}m$)–monoclinic (space group $C2/c$) transition. This is clearly a reconstructive transition. The volume change in the monoclinic (space group $C2/c$)–rhombohedral I (space group $R\bar{3}c$) and rhombohedral I (space group $R\bar{3}c$)–rhombohedral II (space group $R\bar{3}c$) transitions are 3% and 1.5% respectively. The latter transition is more likely to be displacive. The large decrease in volume observed in the cubic to monoclinic transition, as well as the drastic reduction in symmetry, suggest that this is a true first-order transition. The relatively small decrease in volume in the case of the monoclinic to rhombohedral I transition suggests that the space group of the monoclinic phase is a subgroup of $R\bar{3}c$. Jørgensen *et al* [11] observed a 4% relative volume change in the cubic to monoclinic transition, and found the monoclinic to rhombohedral transition to be continuous. A volume decrease of 2–3% was observed by Suzuki *et al* [12] for the cubic II to rhombohedral I transition, and no appreciable change at the rhombohedral I–rhombohedra II transition. From the relative volume versus pressure curves given in figure 5, we find the decompression process to be irreversible. The ReO_3 nanocrystals are stabilized in the metastable monoclinic phase at ambient pressure after decompression.

We have calculated the isothermal bulk modulus, B_0, at ambient pressure and its pressure derivative B_0' for the monoclinic and rhombohedral I phase, by using the Murnaghan equation of state [26]:

$$V/V_0 = [1 + (B_0'/B_0)P]^{-1/B_0'}.$$

Here, V_0 is the volume per formula unit at zero pressure for a particular phase, V being the volume per formula unit at a pressure for that phase. Figures 6(a) and (b) show the relative volume versus pressure curves along with the Murnaghan fit for the monoclinic and the rhombohedral I phases, respectively, in the compression process. As we have only one data point for the cubic and rhombohedral II phases, we could not fit the data to the Murnaghan equation of state. For monoclinic and rhombohedral I phases, we have fitted the experimental data by treating B_0, B_0' and V_0 as refinable parameters (solid lines in figures 6(a) and (b)) or treating B_0 and V_0 as refinable parameters with B_0' constrained (dotted lines in figures 6(a) and (b)) to be equal to four for all phases ($B_0' = 4$ in [11] for bulk ReO_3). With B_0, B_0' and V_0 as refinable parameters, we have estimated their values for the monoclinic and rhombohedral I phases of the nanocrystals to be 31.5 ± 1.7 GPa, 8.67, 50.97 Å^3; and 72.7 ± 3 GPa, 1.36, 49.96 Å^3 respectively. With B_0 and V_0 as refinable parameters and B_0' equal to four, we have estimated the values of B_0 and V_0 for the monoclinic and rhombohedral I phases as 35.8 ± 2 GPa, 50.97 Å^3; and 59.9 ± 3.8 GPa, 49.96 Å^3 respectively. The value of the isothermal bulk modulus B_0 at ambient pressure for the monoclinic phase is less than that of the rhombohedral I phase. By using a Birch-type equation of state with B_0' taken as four, Jørgensen *et al* [11] reported the values of B_0 and V_0 for the monoclinic and rhombohedral I phases to be 96 GPa, 50.23 Å^3; and 129 GPa, 48.6 Å^3 respectively in the case of bulk ReO_3. These results suggest that nanocrystalline ReO_3 is roughly twice as compressible as bulk ReO_3. A similar result has been reported for nanocrystalline α-Fe and Fe_3C inside the multi-walled carbon nanotubes [30].

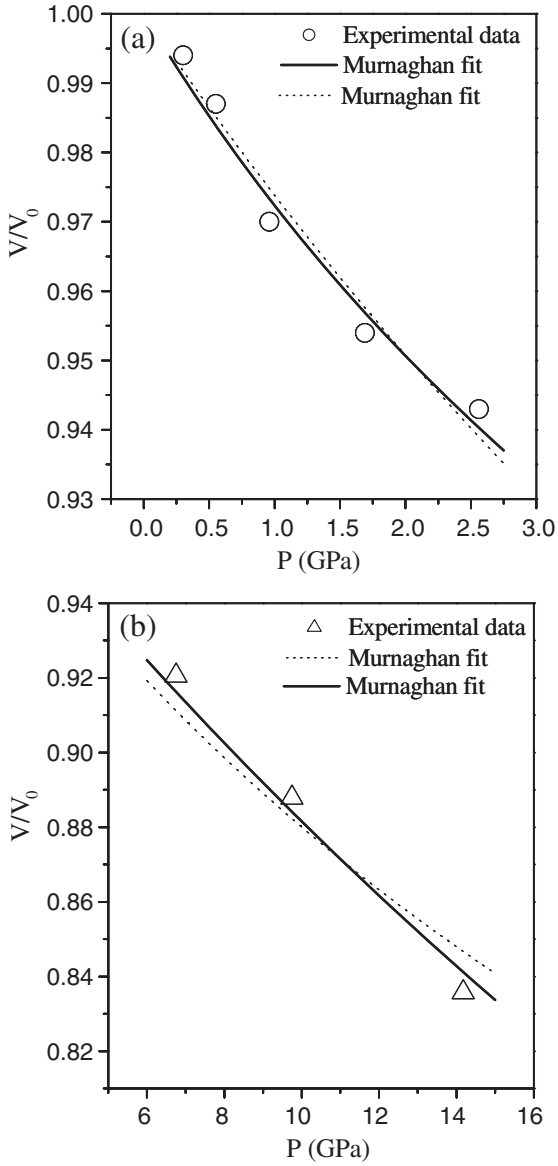

Figure 6. Relative volume versus pressure curves for the (a) monoclinic and (b) rhombohedral I phases of ReO_3 nanocrystals (∼12 nm average diameter). Dotted and solid lines are fits to the Murnaghan equation of state for B_0' constrained to be equal to four and refinable parameters respectively.

4. Conclusions

A synchrotron x-ray investigation of the pressure-induced phase transitions in ReO_3 nanocrystals with an average diameter ∼12 nm has been carried out. The results show that the ambient-pressure cubic I structure (space group $Pm\bar{3}m$) transforms first to a monoclinic structure (space group $C2/c$), and then to a rhombohedral I structure (space group $R\bar{3}c$), and

finally to another rhombohedral phase (rhombohedral II, space group $R\bar{3}c$) with increasing pressure over the 0.0–20.3 GPa range. In table 1, we have given a summary of the structural data on the different phases obtained by us. The surface to volume ratio is very large in nanocrystals and the probability of monodomain crystallites evolves inversely with the size of the nanocrystals. Nanocrystals possess excess surface energy which can play an important role in the stability of crystalline phases. Thus, a high-pressure phase can be stabilized under ambient conditions in nanocrystals. In the present study, the high-pressure monoclinic phase of ReO_3 becomes stabilized under ambient conditions on decompression. Larger hysteresis between the compression and decompression runs is also observed for nanocrystals. Furthermore, the transition pressures of nanocrystals are generally lower than those reported for bulk ReO_3. An examination of the volume changes of the different transitions shows the cubic to monoclinic transition to be of first-order. Interestingly, the ReO_3 nanocrystals are more compressible than the bulk.

Acknowledgments

AKS thanks the Department of Science and Technology, India, for financial support. The work was partially supported by the NSF.

References

[1] Rao C N R and Raveau B 1995 *Transition Metal Oxides* 2nd edn (Weinheim: Wiley–VCH)
[2] Ferretti A, Rogers D B and Goodenough J B 1965 *J. Phys. Chem. Solids* **26** 2007
[3] Razavi F S, Altounian Z and Datars W R 1978 *Solid State Commun.* **28** 217
[4] Schirber J E and Morosin B 1979 *Phys. Rev. Lett.* **42** 1485
[5] Batlogg B, Maines R G and Greenblatt M 1984 *Phys. Rev.* B **29** 3762
[6] Axe J D, Fujii Y, Batlogg B, Greenblatt M and Gregorio S D 1985 *Phys. Rev.* B **31** 663
[7] Schirber J E, Morosin B, Alkire R W, Larson A C and Vergamini P J 1984 *Phys. Rev.* B **29** 4150
[8] Schirber J E and Mattheiss L F 1981 *Phys. Rev.* B **24** 692
[9] Jørgensen J-E, Jorgensen J D, Batlogg B, Remeika J P and Axe J D 1986 *Phys. Rev.* B **33** 4793
[10] Chatterji T and McIntyre G J 2006 *Solid State Commun.* **139** 12
[11] Jørgensen J-E, Olsen J S and Gerward L 2000 *J. Appl. Crystallogr.* **33** 279
[12] Suzuki E, Kobayashi Y, Endo E and Kikegawa T 2002 *J. Phys.: Condens. Matter* **14** 10589
[13] Jørgensen J-E, Marshall W G, Smith R I, Olsen J S and Gerward L 2004 *J. Appl. Crystallogr.* **37** 857
[14] Biswas K and Rao C N R 2006 *J. Phys. Chem.* B **110** 842
[15] Nechamkin H, Kurtz A N and Hiskey C F 1951 *J. Am. Chem. Soc.* **73** 2828
[16] Audrieth L F 1950 *Inorg. Synth.* **3** 187
[17] Mao H K, Bell P M, Shaner J W and Steinberg D J 1978 *J. Appl. Phys.* **49** 3276
[18] Rodríguez-Carvajal J 1990 FULLPROF, A program for Rietveld refinement and pattern matching analysis *Abstracts of the Satellite Mtg on Powder Diffraction of the XV Congr. of the IUCr (Toulouse, France)* p 127
[19] Rodríguez-Carvajal J 1993 *Physica* B **192** 55
[20] LeBail A, Duroy H and Fourquet J L 1988 *Mater. Res. Bull.* **23** 447
[21] Pawley G S 1981 *J. Appl. Crystallogr.* **14** 357
[22] Edreva-Kardzhieva R and Andreev A A 1977 *Z. Neorg. Khim.* **22** 2007
[23] Ghosh M, Sampathkumaran E V and Rao C N R 2005 *Chem. Mater.* **17** 2348
[24] Ghosh M, Biswas K, Sundaresan A and Rao C N R 2006 *J. Mater. Chem.* **16** 106
[25] Schrötter F and Müller B G 1993 *Z. Anorg. Allg. Chem.* **619** 1426
[26] Jack K H and Gutmann V 1951 *Acta Crystallogr.* **4** 246
[27] Seo W S, Shim J H, Oh S J, Lee E K, Hur N H and Park J T 2005 *J. Am. Chem. Soc.* **127** 6188
[28] Gautam U K, Seshadri R and Rao C N R 2003 *Chem. Phys. Lett.* **375** 560
[29] Murnaghan F D 1944 *Proc. Natl Acad. Sci. USA* **30** 244
[30] Karmakar S, Sharma S M, Teredesai P V and Sood A K 2004 *Phys. Rev.* B **69** 165414